SAND2019-4893J

On the Design of Sinuous Antennas for UWB Radar Applications

Dylan A. Crocker *Student, IEEE* and Waymond R. Scott, Jr., *Fellow, IEEE*

***Abstract*—Sinuous antennas are capable of producing ultra-wideband radiation with polarization diversity. This capability makes the sinuous antenna an attractive candidate for UWB polarimetric radar applications. Additionally, the ability of the sinuous antenna to be implemented as a planar structure makes it a good fit for close in sensing applications such as ground penetrating radar. However, recent literature has shown the sinuous antenna to suffer from resonances which degrade performance. Such resonances produce late time ringing which is particularly troubling for pulsed close in sensing applications. The resonances occur in two forms: log-periodic resonances on the arms, and a resonance due to the sharp ends left by the outer truncation. A detailed investigation as to the correlation between the log-periodic resonances and the sinuous antenna design parameters indicates the resonances may be mitigated by selecting appropriate design parameters. In addition, a novel truncation method is proposed to remove the sharp end resonance. Both simulation and measured results are provided to support the developed sinuous antenna design guidance.**

***Index Terms*—Antennas, broadband antennas, ground penetrating radar, radar antennas, sinuous antennas.**

I. Introduction

The sinuous antenna was first published in a patent by DuHamel in 1987. The patent describes the sinuous antenna as a combination of spiral and log-periodic antenna concepts which resulted in a design capable of producing ultra-wideband (UWB) radiation with polarization diversity [1]. Such attributes have made the sinuous antenna useful in direction finding [2], [3], human health monitoring [4], radio astronomy [5]–[8], terahertz detectors [9]–[12], electromagnetic pulse (EMP) [13], and other UWB applications.

The use of sinuous antennas in polarimetric radar systems [14] is especially intriguing due to the ability of the four-arm sinuous antenna to produce dual-polarized radiation over wide bandwidths. Other wideband antenna designs such as quad-ridge horn [15], Vivaldi [16], and resistive-vee [17] antennas provide similar capabilities. However, they require relatively large and often complex three dimensional structures in order to produce orthogonal senses of polarization. Alternatively, the sinuous antenna may be implemented as a planar structure. The combination of polarimetric capabilities with a low profile make the sinuous antenna attractive to close-in sensing applications such as ground penetrating radar (GPR).

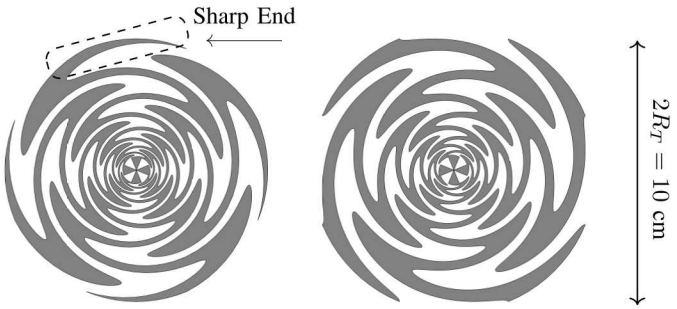

Fig. 1. Illustration of sinuous antenna designs. Left: Reference Design (8 cells, $\tau = 0.75$, $\alpha = 60°$, $R_T = 5$ cm, with traditional truncation). Right: Improved Design (8.5 cells, $\tau = 0.7628$, $\alpha = 45°$, $R_T = 5$ cm, with the new truncation). Note: the two designs have the same outer radius.

Although sinuous antennas provide the desirable properties described above, the antennas can suffer from unintended resonances which degrade performance. The sharp ends produced by the outer truncation (see Fig. 1) of the antenna have been shown to resonate when their length is approximately $\lambda/2$ which produces both pattern distortion and ringing in the time domain [18]–[21]. Further, log-periodic resonances occurring internal to the sinuous arms have been observed and shown to produce additional ringing as well as deleterious effects on gain smoothness, polarization purity, and group delay [21], [22]. Such resonances may reduce the effectiveness of sinuous antennas, particularly when applied to sensing applications which transform the data into the time domain. However, techniques for their mitigation have been presented in the literature. The sharp ends may be empirically removed in order to prevent the associated resonance [6], [18]–[24]. Similarly, in [21], [22] the sinuous cell tips were clipped along the antenna arm in order to mitigate the log-periodic resonances. While these techniques have been successful, they require additional empirical design steps while destroying the self-complimentary nature of the antenna—reducing both elegance and frequency independence.

In this work, a detailed investigation as to the correlation between the log-periodic resonances and the sinuous antenna design parameters will be presented. It will be shown that these resonances may be mitigated simply by selecting appropriate

This work was supported by the U.S. Army CCDC C5ISR Center, Night Vision and Electronic Sensors Directorate, Countermine Division, Countermine Technologies Branch; the U.S. Army Research Office under Grant Number W911NF-11-1-0153; and by Sandia National Laboratories, a multimission laboratory managed and operated by National Technology and Engineering Solutions of Sandia, LLC., a wholly owned subsidiary of Honeywell International, Inc., for the U.S. Department of Energy's National Nuclear Security Administration under contract DE-NA0003525. This paper describes objective technical results and analysis. Any subjective views or opinions that might be expressed in the paper do not necessarily represent the views of the U.S. Department of Energy or the United States Government.

D. A. Crocker is with Sandia National Laboratories, Albuquerque, NM 87123 USA.

W. R. Scott, Jr., is with the Georgia Institute of Technology, Atlanta, GA 30332 USA.

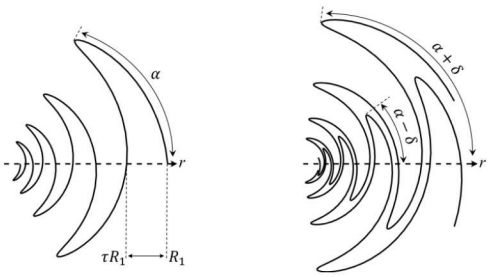

Fig. 2. Illustration of sinuous antenna design parameters: angular width α, expansion ratio τ, outermost cell radius R_1, and curve rotation angle δ.

design parameters. In addition, a novel truncation method is proposed to remove the sharp-end resonance. Measured data is provided in order to validate the developed design guidance.

II. Simulations

A. Sinuous Antenna Geometry

Sinuous antennas are comprised of N arms each made up of P cells where the curve of the p^{th} cell is described in polar coordinates (r, ϕ) by

$$\phi = (-1)^{p-1}\alpha_p \sin\left(\frac{\pi \ln(r/R_p)}{\ln(\tau_p)}\right) \pm \delta, \qquad (1)$$

where $R_{p+1} \leq r \leq R_p$ [1]. In (1), R_p controls the outer radius, τ_p the growth rate i.e., $R_{p+1} = \tau R_p$, and α_p the angular width of the p^{th} cell. The curve is then rotated by the angles $\pm\delta$ in order to fill out the arm. The design parameters are illustrated in Fig. 2. In this analysis, four-arm ($N = 4$) sinuous antennas are considered with τ, α, and δ constant for all cells which produces log-periodic structures [1], [25]. Additionally, δ is set to 22.5° for all antennas considered in order to produce self-complementary structures[1]. The self-complementary condition helps ensure that the sinuous antenna's input impedance is both real and frequency independent [26]. The antenna is fed by a self-complimentary arrangement of orthogonal bow-tie elements each feeding a set of opposing sinuous arms.

B. Resonances

In order to investigate the resonances, a full-wave electromagnetic analysis of the sinuous antenna in free-space was conducted using the CST Microwave Studio [27] time-domain solver. Both pairs of opposing sinuous arms were terminated by an ideal port set to the theoretical impedance of 267 Ω [26]. A single pair was then driven, with the other pair remaining matched, in order to produce linearly polarized radiation. The resulting co-polarized realized gain and group delay are shown in Fig. 3 (Reference Design) and display prominent resonances. The resonance at approximately 1.7 GHz is attributed to the sharp-ends of the antenna [21] and will be removed by the outer truncation discussed in section II-D.

[1]A structure is considered self-complimentary when the metal and non-metal sections are exact replicas offset by a rotation. For sinuous antennas defined by (1), the self-complimentary condition is met when $\delta = 90°/P$. The parameter α does not affect this condition as only δ controls the metal to non-metal ratio.

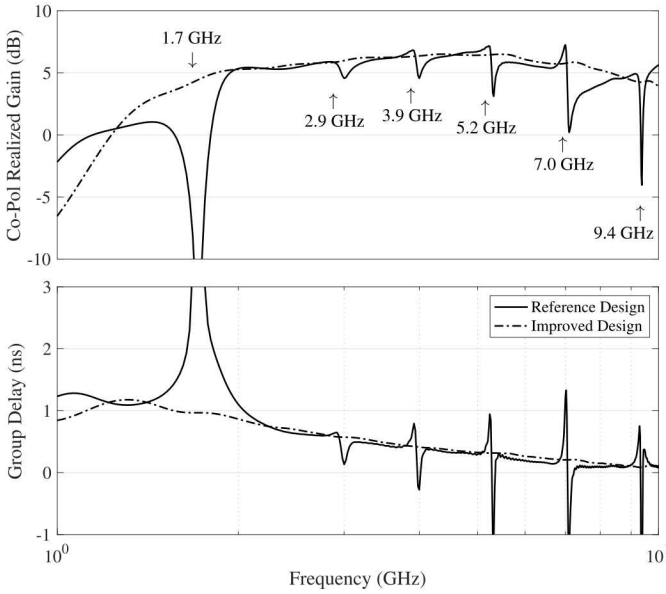

Fig. 3. Co-polarized realized gain (logarithmic frequency scale) of sinuous antennas: Reference Design (8 cells, $\tau = 0.75$, $\alpha = 60°$, $R_T = 5$ cm, with traditional truncation) and Improved Design (8.5 cells, $\tau = 0.7628$, $\alpha = 45°$, $R_T = 5$ cm, with new truncation).

The additional resonances starting at 2.9 GHz are log-periodic in frequency and attributed to interactions between adjacent arms. It will be shown in section II-C that these interactions may be mitigated by reducing the interleaving of adjacent arms i.e., smaller values of α.

C. Parametric Study

A parametric study of both the angular width α and expansion ratio τ was conducted in order to determine correlation with the log-periodic resonances. The study resulted in a large amount of data which motivated the development of a *gain smoothness metric* for quantifying the effectiveness of each parameter combination at mitigating the log-periodic resonances. The metric M is the root-mean-squared error between the co-polarized realized gain and its N-point simple moving average as

$$M = \sqrt{\frac{1}{N}\sum_{f_n=f_s}^{f_e}\left(|G(f_n)| - \frac{1}{N}\sum_{k=n-N/2}^{n+N/2}|G(f_k)|\right)^2}, \qquad (2)$$

where in this case $f_{start} \approx 3$ GHz, $f_{stop} = 10$ GHz and $N = 31$ (600 MHz wide). The actual starting frequency was adjusted for each design to ensure all the log-periodic resonances were included and not the resonance due to the sharp end. The results of the metric are shown in Fig. 4 and indicate that the gain *smoothness* converges at approximately $\alpha = 45°$ for all values of τ.

Although decreasing α to $\leq 45°$ may produce smooth radiation over wide bandwidths, the overall length of the sinuous antenna arms are decreased thus negatively impacting the low-frequency operation of the antenna. The lowest frequency

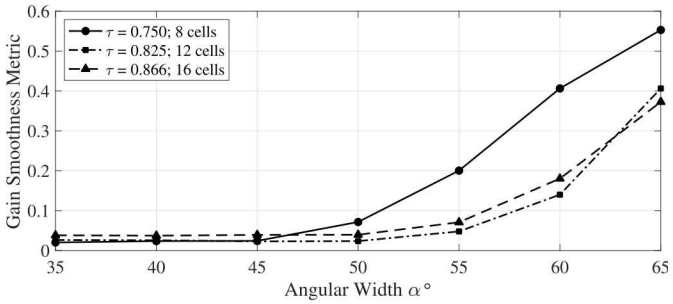

Fig. 4. Gain smoothness metric M computed for the parametric study which shows distortion of gain over frequency increases with α. For this study, the value of α was swept from 35° to 65° in 5° increments for three values of τ (0.75, 0.825, and 0.866) while keeping all other design parameters constant.

of operation is inversely proportional to α by the following approximate relation

$$f_{lo} = \frac{v}{4R_T(\alpha + \delta)}, \tag{3}$$

where v is the wave velocity and α and δ are specified in radians [1]. For applications desiring smooth gain in addition to low-frequency operation, $\alpha = 50°$ may be used with a larger τ. The results in Fig. 4 indicate $\tau = 0.825$ to be optimal. Although, other performance trade-offs must be considered with larger values of τ such as increased dispersion and conductor losses [28].

D. Outer Truncation

Traditionally, sinuous antennas have been truncated in a circle of radius R_T applied at the end of the last cell i.e., $R_T = R_1$. This truncation method produces a sharp end, as shown in Fig. 1, that resonates when its length is approximately $\lambda/2$. In [18]–[21] this resonance is mitigated by clipping off the sharp ends; however, a new technique is presented here that simply changes the circular truncation radius R_T to the tip of the outermost cell (i.e., $R_T = \sqrt{\tau}R_1$), as illustrated by the antenna on the right in Fig. 1. This technique mitigates the resonance as the sharp ends are no longer produced. Additionally, the self-complementary nature of the antenna is maintained.

E. Improved Design

Utilizing the design guidance developed herein, a sinuous antenna was developed to produce smooth radiation over UWB frequency. The value of α is chosen as 45° in order to prevent the log-periodic resonances while the outer region is truncated by the new method proposed above. Both τ and R_1 have been adjusted to 0.7628 and 5.72 cm respectively in order for the truncation radius to be equal to the outer radius of the reference design. In addition, the radius of the bowtie element feed is kept to a constant 0.5 cm. The number of cells P is increased by one to have the same number of complete cells when the circular truncation is applied to the outermost cell tip. From the results presented in Fig. 4, one might have based the improved design on the 12 cell ($\tau = 0.825$) antenna with 50° angular width; however, for comparison purposes, particularly in the time-domain, the improved design was kept as close to the reference as possible. The simulated realized gain and group delay are plotted in Fig. 3 (Improved Design) and show the resonances have been successfully mitigated. The resonance at 1.7 GHz was mitigated by the new truncation method while the log-periodic resonances were mitigated by the selection of α. The smooth gain and corresponding smooth group delay prevents ringing in the time domain when utilized for pulsed UWB applications.

F. Time-Domain Analysis

Distortion in the gain of the sinuous antenna—due to the resonances—ultimately results in ringing when the antenna is used in pulsed type applications. This can be particularly troublesome for close-in sensing applications such as GPR. Examination of the radiated fields in the time domain is necessary to determine the extent of such ringing. Fig. 5 shows the radiated pulses at 2 m for the sinuous antennas investigated when driven by an UWB pulse. The excitation pulse used was a Differentiated Gaussian which is defined by

$$v_{pulse}(t) = -v_{peak}\frac{(t-\mu)}{\sigma}\exp\left[0.5 - \frac{(t-\mu)^2}{2\sigma^2}\right], \tag{4}$$

where μ represents an arbitrary time shift and σ, defined as $2.3548/(2\pi f_{BW})$, controls the width of the pulse. In the presented analysis v_{peak} was set to 1 V and f_{BW} to 7.5 GHz resulting in peak spectral energy at 3.2 GHz. The radiated pulses shown in Fig. 5 do not have the shape described in (4), this is due to dispersion. Compensation of dispersion in sinuous antennas is a topic of future research.

As shown in Fig. 5, the resonances present in the reference antenna radiation produce high frequency ringing following the pulse in time. Mitigation of the frequency domain resonances eliminates the time domain ringing as illustrated by the improved design. Note that the improved design has a slightly different pulse shape, compared to the reference design, due to the change in τ. The improved design is able to produce smooth radiation merely by selecting the appropriate angular width and outer truncation.

III. Measurements

A. Antenna Fabrication

In order to provide experimental validation for the previous analysis conducted through simulation, both the reference and improved designs (described above) were fabricated and measured. The antennas were produced by an LPKF PCB milling machine [29] out of 0.062" Rogers RT/duroid® 5880 laminate (0.5 oz. copper clad). The 5880 material has very low loss (tanδ of 0.0009 at 10 GHz) and a relative permittivity ε_r of 2.20 [30]. The fabricated antennas are shown in Fig. 6. As can be seen, each set of opposing sinuous arms were placed on opposite sides of the substrate. This was done in order to simplify feeding the antennas. Since linear polarization was desired for the validation measurements, only a single pair of arms were fed by a tapered microstrip balun while the other pair of arms were terminated with a 215Ω chip resistor [31], [32]. Simulation results showed the presence of the substrate lowered the input impedance to approximately 215Ω (averaged

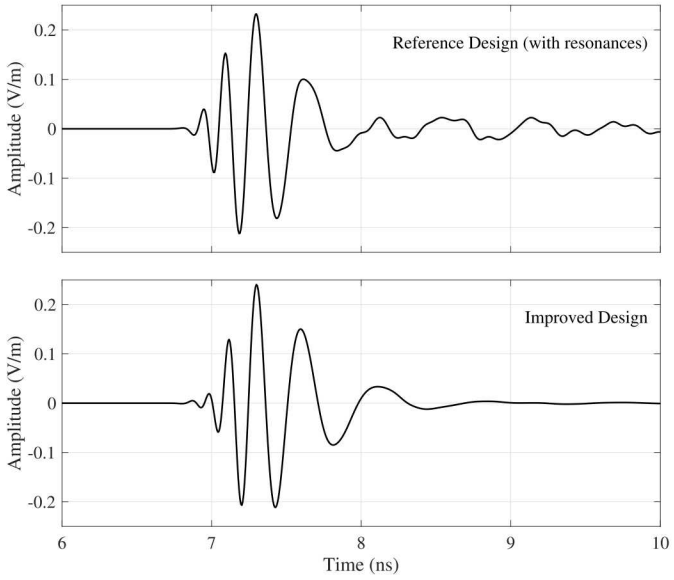

Fig. 5. Comparison of radiated pulses at 2 m (boresight) for Reference Design (with resonances) and Improved Design (without resonances). Note the significant late time ringing present in the Reference Design.

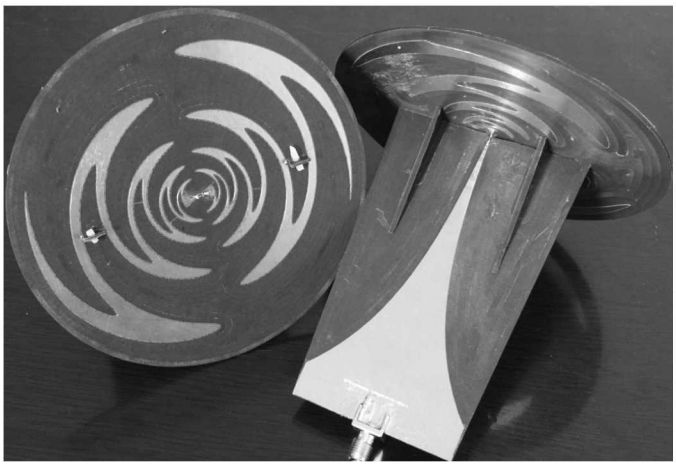

Fig. 6. Fabricated sinuous antennas: reference (left) and improved design (right).

over the band). The constructed balun started as unbalanced 50Ω microstrip which was then tapered over a 90 mm length to balanced 215Ω parallel stripline. The top trace was tapered linearly while an exponential taper was used for the ground plane (pictured in Fig. 6). The microstrip was fed by an SMA edge connector. For structural stability, triangular braces were included (also cut from the 5880 material) and the balun had tabs that extended through slots cut into the antenna substrate allowing plastic pins to hold the parts together.

B. Results

The antenna patterns were measured using an MVG StarLab near-field measurement system [33]. Full models of the measured antennas (including the SMA transition) were developed in CST and simulated using the time-domain solver. The simulated and measured realized gains of the reference and

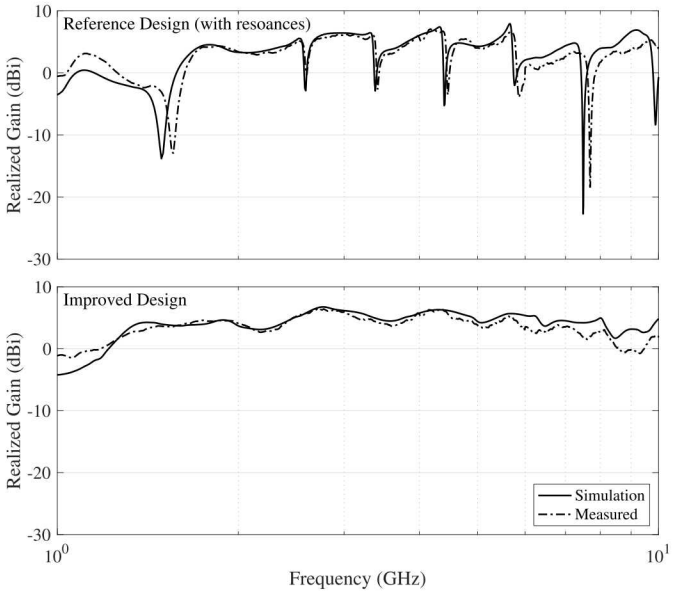

Fig. 7. Measured and simulated co-polarized realized gain of the fabricated antennas: reference design (top) and improved design (bottom). Simulation results are overlayed as the dashed line.

improved designs are shown in Fig. 7. As can be seen, the simulated and measured results correlate very well from 2 to 6 GHz. At the lower and higher frequencies some relatively small discrepancies are observed. This is not surprising since the antenna is not well matched below 2 GHz and at higher frequencies the coarseness of the mesh as well as fabrication imperfections start to have an effect. However, the presence and mitigation of the resonances in the gain are unmistakably clear. Also, note that the presence of the substrate shifts the resonances observed down in frequency from that shown in Fig. 3.

IV. Summary

In this letter, an analysis of the relationship between the sinuous antenna design parameters and resonances producing distortion in the radiation was presented. It was determined that the resonances may be eliminated by proper selection of both the design parameters and outer truncation method. The optimal value of α was slightly impacted by the choice of expansion ratio τ but converged at approximately 45° for all the designs investigated. These results are corroborated by design guidance provided in [34]. Mitigation of the resonances by the proposed techniques provide advantages over those proposed in the literature [18]–[22] since the antenna remains self-complimentary and does not require additional, empirical, design steps i.e., trimming.

Acknowledgment

The authors would like to thank B. Strassner II, D. Brown, J. Borchardt, T. Satterthwait, W. Freeman and W. Patitz of Sandia National Laboratories for helpful discussion and feedback during the development of this paper as well as assistance in the use of the fabrication and measurement equipment.

REFERENCES

[1] R. H. DuHamel, "Dual polarized sinuous antennas," Apr. 14 1987, US Patent 4,658,262.

[2] H. S. Zhang, K. Xiao, L. Qiu, and S. L. Chai, "Four-arm sinuous antenna for direction finding system," in *2014 IEEE International Wireless Symposium (IWS 2014)*, March 2014, pp. 1–4.

[3] A. Bellion, C. L. Meins, A. Julien-Vergonjanne, and T. Monediere, "A new compact dually polarized direction finding antenna on the uhf band," in *2008 IEEE Antennas and Propagation Society International Symposium*, July 2008, pp. 1–4.

[4] C. Xu, F. lina, W. Xianfeng, and H. Chunjiu, "Design of an ultra-wideband sinuous antenna applied for respiratory monitor," in *2016 Asia-Pacific International Symposium on Electromagnetic Compatibility (APEMC)*, vol. 01, May 2016, pp. 256–258.

[5] R. S. Gawande and R. F. Bradley, "G/t sensitivity comparison of different topologies using ultra wide band, active, conical sinuous antenna," in *2009 IEEE Antennas and Propagation Society International Symposium*, June 2009, pp. 1–4.

[6] R. Gawande and R. Bradley, "Towards an ultra wideband low noise active sinuous feed for next generation radio telescopes," *IEEE Transactions on Antennas and Propagation*, vol. 59, no. 6, pp. 1945–1953, June 2011.

[7] M. V. Ivashina, R. Bradley, R. Gawande, M. Pantaleev, B. Klein, J. Yang, and C. Bencivenni, "System noise performance of ultra-wideband feeds for future radio telescopes: Conical-sinuous antenna and eleven antenna," in *2014 XXXIth URSI General Assembly and Scientific Symposium (URSI GASS)*, Aug 2014, pp. 1–4.

[8] D. I. L. de Villiers, "Initial study of a pyramidal sinuous antenna as a feed for the ska reflector system in band-1," in *2017 IEEE International Symposium on Antennas and Propagation USNC/URSI National Radio Science Meeting*, July 2017, pp. 555–556.

[9] L. Liu, H. Xu, R. R. Percy, D. L. Herald, A. W. Lichtenberger, J. L. Hesler, and R. M. Weikle, "Development of integrated terahertz broadband detectors utilizing superconducting hot-electron bolometers," *IEEE Transactions on Applied Superconductivity*, vol. 19, no. 3, pp. 282–286, June 2009.

[10] L. Liu, J. L. Hesler, H. Xu, A. W. Lichtenberger, and R. M. Weikle, "A broadband quasi-optical terahertz detector utilizing a zero bias schottky diode," *IEEE Microwave and Wireless Components Letters*, vol. 20, no. 9, pp. 504–506, Sept 2010.

[11] O. Y. Volkov, Y. Y. Divin, V. N. Gubankov, I. I. Gundareva, and V. V. Pavlovskiy, "Spectral analysis of subterahertz resonant system by josephson admittance spectroscopy," in *35th International Conference on Infrared, Millimeter, and Terahertz Waves*, Sept 2010, pp. 1–2.

[12] Z. Jiang, S. M. Rahman, P. Fay, S. T. Ruggiero, and L. Liu, "Lens-coupled dual polarization sinuous antenna for quasi-optical terahertz balanced mixers," in *2012 Asia Pacific Microwave Conference Proceedings*, Dec 2012, pp. 52–54.

[13] A. H. Stults, "Impulse loading of sinuous antennas by ferroelectric generators," in *2008 IEEE International Power Modulators and High-Voltage Conference*, May 2008, pp. 156–158.

[14] D. Giuli, "Polarization diversity in radars," *Proceedings of the IEEE*, vol. 74, no. 2, pp. 245–269, Feb 1986.

[15] D. J. Blejer, S. M. Scarborough, C. E. Frost, H. R. Catalan, K. H. McCoin, J. Roman, and D. M. Mukai, "Ultra-wideband polarimetric imaging of corner reflectors in foliage," in *IEEE Antennas and Propagation Society International Symposium 1992 Digest*, June 1992, pp. 587–590 vol.1.

[16] G. P. Pochanin, N. M. Kaluzhny, S. A. Masalov, and I. Y. Pochanina, "Ultrawideband linearly polarized antennas of vivaldi type for ground penetrating radar," in *2015 International Conference on Antenna Theory and Techniques (ICATT)*, April 2015, pp. 1–3.

[17] J. W. Sustman and W. R. Scott, "A resistive-vee dipole based polarimetric antenna," in *2013 IEEE Antennas and Propagation Society International Symposium (APSURSI)*, July 2013, pp. 888–889.

[18] K. S. Saini and R. F. Bradley, "The sinuous antenna-a dual polarized element for wideband phased array feed application," *NRAO Electronics Division Internal Memo no. 301*, p. 5, 1996.

[19] Y. Kang and K. Kim, "Experimental validation of removal of sharp ends in sinuous antenna arms," in *2013 Asia-Pacific Microwave Conference Proceedings (APMC)*, Nov 2013, pp. 212–214.

[20] ——, "Investigation of the effects of sharp-ends removal in the sinuous antenna arms on the radiation patterns," in *2015 IEEE International Symposium on Antennas and Propagation USNC/URSI National Radio Science Meeting*, July 2015, pp. 1989–1990.

[21] Y. Kang, K. Kim, and W. R. Scott, "Modification of sinuous antenna arms for uwb radar applications," *IEEE Transactions on Antennas and Propagation*, vol. 63, no. 11, pp. 5229–5234, Nov 2015.

[22] Y. Kang and K. Kim, "Polarization improvement through sinuous antenna arm modification," in *2016 International Symposium on Antennas and Propagation (ISAP)*, Oct 2016, pp. 386–387.

[23] H. R. Fang, R. Balakrishnan, R. Guinvarc'h, and K. Mouthaan, "Quad-polarized wideband phased array with reduced sidelobes by interstitial-packing," in *2015 9th European Conference on Antennas and Propagation (EuCAP)*, May 2015, pp. 1–5.

[24] I. M. Alotaibi, J. Hong, and S. K. Almorqi, "Cavity-backed dual linear polarization sinuous antenna with integrated microstrip balun feed," in *2015 IEEE 15th Mediterranean Microwave Symposium (MMS)*, Nov 2015, pp. 1–4.

[25] R. DuHamel and D. Isbell, "Broadband logarithmically periodic antenna structures," in *1958 IRE International Convention Record*, vol. 5, March 1957, pp. 119–128.

[26] J. M. Edwards, R. O'Brient, A. T. Lee, and G. M. Rebeiz, "Dual-polarized sinuous antennas on extended hemispherical silicon lenses," *IEEE Transactions on Antennas and Propagation*, vol. 60, no. 9, pp. 4082–4091, Sept 2012.

[27] Computer Simulation Technology, "CST Microwave Studio." [Online]. Available: https://www.cst.com/products/cstmws

[28] P. Baldonero, A. Manna, F. Trotta, A. Pantano, and M. Bartocci, "UWB Double polarised phased array," in *2009 3rd European Conference on Antennas and Propagation*, March 2009, pp. 556–560.

[29] LPKF Laser & Electronics AG, "LPKF Laser & Electronics," https://www.lpkf.com/en/, accessed: 2019-01-29.

[30] Rogers Corporation, "RT/duroid 5880 Laminates," http://www.rogerscorp.com/acs/products/32/rt-duroid-5880-laminates.aspx, accessed: 2019-01-29.

[31] N. Lorho, G. Lirzin, A. Bikiny, S. Lestieux, A. Chousseaud, and T. Razban, "Miniaturization of an uwb dual-polarized antenna," in *2015 IEEE International Conference on Ubiquitous Wireless Broadband (ICUWB)*, Oct 2015, pp. 1–5.

[32] K. M. P. Aghdam, R. Faraji-Dana, and J. Rashed-Mohassel, "Optimization of microstrip tapered balun for sinuous antenna feeding circuits," in *2004 10th International Symposium on Antenna Technology and Applied Electromagnetics and URSI Conference*, July 2004, pp. 1–4.

[33] MVG, "StarLab," https://www.mvg-world.com/en/products/field_product_family/antenna-measurement-2/starlab, accessed: 2019-01-29.

[34] R. H. DuHamel and J. P. Scherer, "Frequency-independent antennas," in *Antenna Engineering Handbook*, 3rd ed., R. C. Johnson and H. Jasik, Eds. New York: McGraw-Hill, 1993, ch. 14.